

Received December 23, 2020, accepted January 15, 2021, date of publication January 19, 2021, date of current version February 1, 2021.

Digital Object Identifier 10.1109/ACCESS.2021.3052835

Diagnosing Coronavirus Disease 2019 (COVID-19): Efficient Harris Hawks-Inspired Fuzzy K-Nearest Neighbor Prediction Methods

HUA YE¹, PEILIANG WU², TIANRU ZHU³, ZHONGXIANG XIAO⁴, XIE ZHANG¹, LONG ZHENG¹, RONGWEI ZHENG⁵, YANGJIE SUN¹, WEILONG ZHOU¹, QINLEI FU¹, XINXIN YE¹, ALI CHEN¹, SHUANG ZHENG¹, ALI ASGHAR HEIDARI^{6,7}, MINGJING WANG⁸, JIANDONG ZHU⁹, HUILING CHEN¹⁰, (Associate Member, IEEE), AND JIFA LI¹

¹Department of Pulmonary and Critical Care Medicine, Affiliated Yueqing Hospital, Wenzhou Medical University, Yueqing 325600, China

²Department of Pulmonary and Critical Care Medicine, The 1st Affiliated Hospital, Wenzhou Medical University, Wenzhou 325000, China

³The Second Clinical College, Wenzhou Medical University, Wenzhou 325000, China

⁴Department of Pharmacy, Affiliated Yueqing Hospital, Wenzhou Medical University, Yueqing 325600, China

⁵Department of Urology, Affiliated Yueqing Hospital, Wenzhou Medical University, Yueqing 325600, China

⁶School of Surveying and Geospatial Engineering, College of Engineering, University of Tehran, Tehran 1417466191, Iran

⁷Department of Computer Science, School of Computing, National University of Singapore, Singapore 117417

⁸Institute of Research and Development, Duy Tan University, Da Nang 550000, Vietnam

⁹Department of Surgical Oncology, Affiliated Yueqing Hospital, Wenzhou Medical University, Yueqing 325600, China

¹⁰College of Computer Science and Artificial Intelligence, Wenzhou University, Wenzhou 325035, China

Corresponding authors: Jifa Li (ljf58800@163.com), Huiling Chen (chenhuiling.jlu@gmail.com), and Jiandong Zhu (873331666@qq.com)

ABSTRACT This study is devoted to proposing a useful intelligent prediction model to distinguish the severity of COVID-19, to provide a more fair and reasonable reference for assisting clinical diagnostic decision-making. Based on patients' necessary information, pre-existing diseases, symptoms, immune indexes, and complications, this article proposes a prediction model using the Harris hawks optimization (HHO) to optimize the Fuzzy K-nearest neighbor (FKNN), which is called HHO-FKNN. This model is utilized to distinguish the severity of COVID-19. In HHO-FKNN, the purpose of introducing HHO is to optimize the FKNN's optimal parameters and feature subsets simultaneously. Also, based on actual COVID-19 data, we conducted a comparative experiment between HHO-FKNN and several well-known machine learning algorithms, which result shows that not only the proposed HHO-FKNN can obtain better classification performance and higher stability on the four indexes but also screen out the key features that distinguish severe COVID-19 from mild COVID-19. Therefore, we can conclude that the proposed HHO-FKNN model is expected to become a useful tool for COVID-19 prediction.

INDEX TERMS COVID-19, coronavirus, fuzzy K-nearest neighbor, Harris hawk optimization, disease diagnosis, feature selection.

I. INTRODUCTION

Coronavirus disease 2019 (COVID-19) is a highly contagious viral disease, and the World Health Organization (WHO) declared that the COVID-19 was an international public health emergency [1], [2]. First described COVID-19 in December 2019 in Wuhan, Hubei Province, China. The ongoing outbreak of COVID-19 is affecting multiple countries in the world [1]. Until Mar 11th, 2020,

The associate editor coordinating the review of this manuscript and approving it for publication was Juan Wang.

118,326 cases of COVID-19 were diagnosed worldwide, including 80,955 cases in China and 37,371 cases outside China. Additionally, 4,292 deaths have been triggered by COVID-19 [3]. Many countries are facing increased pressures on health care resources. Up to now, a great deal of studies is focused on using traditional statistical methods to identify risk factors of COVID-19 patients. As an example, older age, pre-existing diseases, abnormal liver function, and T-lymphocyte count were correlated closely with COVID-19 progression and prognosis [4]–[6]. However, traditional statistical methods could not rapidly identify changes

in COVID-19 patient's status during the outbreak. Therefore, there is a crucial need to progress a useful forecasting tool for COVID-19 and quickly categorize illness severity.

Currently, the importance of computational, mathematical, and surveillance-based methods for the study of infectious diseases continues to increase [7]. Machine learning-based methods are increasingly being used to diagnose disease, develop prediction models, and identify risk factors [8]. The benefits of machine learning include improving health professionals' ability to establish diagnosis or prognosis; it will replace much of the work of radiologists and anatomic/clinical pathologists; it will improve the accuracy of diagnosis [9]. Therefore, machine learning is an indispensable tool for clinicians seeking to understand patient-individualized treatment better. We use a machine learning strategy to identify COVID-19 patients at high risk for severe illness and prioritize their hospitalization. It may contribute to reduce patient mortality and reduce the burden on healthcare resources.

Optimization depends on the form of the problem we deal with. It is almost possible to reach any form according to the decision-makers preferences. These problems can be modeled as many-objective [10], [11], memetic [12], robust [13], multiobjective [14], large scale [15], [16], fuzzy [17], and single-objective optimization. These forms and the growing demand for their solvers have raised many challenges in data science. Core problems demanding optimization are not limited to healthcare systems, but technologies such as the neural networks [18], water-energy optimization [19], image boost optimization [20], decision-making systems [21]–[23], temperature optimization [24], deployment optimization in sensor networks [25], sustainable development [26]–[28], parameter optimization [29], optimal resource allocation [30], deep learning tasks [31]–[33], mechanical parameters optimization [34], and many other potentials and connected domains [35]–[39]. One of the main classes are solvers with an evolutionary basis. This optimization algorithm works based on an evolving swarm with stochastic updating rules. They have found a good application effect in many scenarios [40]–[45]. At present, as a new single-objective algorithm, Harris Hawks Optimizer (HHO)¹ has been widely concerned like other optimizers and their applications such as Particle Swarm Optimizer (PSO) [46], [47], Whale Optimizer (WOA) [48], Differential Search (DS) [49], Differential Evolution (DE) [50], Slime Mould Algorithm (SMA)² [51], Monarch Butterfly Optimization (MBO) [52], and Moth Search Algorithm (MSA) [53].

HHO not only has strong plasticity but also has been widely used in other fields. Many HHO variants have been proposed recently [54]–[57]. Elaziz *et al.* [58] proposed an improved Harris-Hawks Optimizer (HHO) to solve a multilevel image segmentation problem's global optimization problem and determine the optimal threshold. A large number

of results and comparisons show that SSA has a strong ability to improve HHO. Gupta *et al.* [59] put four effective strategies into the traditional HHO, such as putting forward a nonlinear prey energy parameter, different fast diving, greedy selection mechanism, and learning based on opposites. Experimental results show that the proposed m-HHO can be a useful optimization tool for solving global optimization problems. Shao, Shao *et al.* [60] proposed a new rolling bearing fault diagnosis method based on variational mode decomposition (VMD), time-shifting multiscale discrete entropy (TSMDE), and support vector machine (SVM) optimized by vibration Harris Hawks Optimization algorithm. The outcomes show that this routine has better diagnostic performance than other comparison methods. Tikhamarine *et al.* [61] Combined multilayer perceptron (MLP) neural network and least squares support vector machine (LSSVM) data-driven technology with advanced natural heuristic optimizer (HHO) to simulate rainfall-runoff relationship. The experimental results show that the mixture of HHO and LSSVM can obtain high accuracy of runoff prediction.

Machine learning is widely used in the medical field. For example, Abbasi *et al.* [62] proposed a new method for solving large-scale stochastic operation optimization problems (SOPs) using a machine learning model and applying the proposed decision-making method of blood unit transportation in the hospital network. The results show that compared with the current strategy, the average daily cost is reduced by 29% with the trained neural network model. In comparison, the average daily cost can be reduced by 37% with the proper optimal strategy. Amiri *et al.* [63] used photonic crystal structure and machine learning technology to calculate the concentration of potassium chloride, urea, and glucose (PUG) in human blood to achieve accurate measurement. Moreover, at this article's finale, a mathematical model is revealed to obtain the output power and potassium chloride changes, urea, and glucose concentrations. Ayyıldız and Arslan Tuncer [64] used red blood cell index and machine learning technology, including support vector machine (SVM) and k-nearest neighbor (KNN), to differentiate IDA from \hat{I} - thalassemia. Instead, it employs the neighborhood component analysis feature selection (NCA) technique to select the dataset's features. Their obtained results point to that the RBC indices can result in higher efficacy than those described in the other works. Banerjee *et al.* [65] used machine learning (ML), artificial neural network (ANN) [18], and a humble statistical test to recognize sars-cov-2 positive patients. This new method can significantly improve initial screening for patients with limited PCR based diagnostic tools. Rammurthy and Mahesh [66] designed the WHHO by combining whale optimization algorithm (WOA) with HHO. They applied it to the tumor automatic classification model. Experiments show that the method of deep CNN based on WHHO is better than other methods.

This study aims to develop efficient frameworks using the Harris hawk's optimizer (HHO), which trains a fuzzy k-nearest neighbor (FKNN) model. Then, the optimized

¹Download the codes at <https://aliasgharheidari.com/HHO.html>

²Download the codes at <https://aliasgharheidari.com/SMA.html>

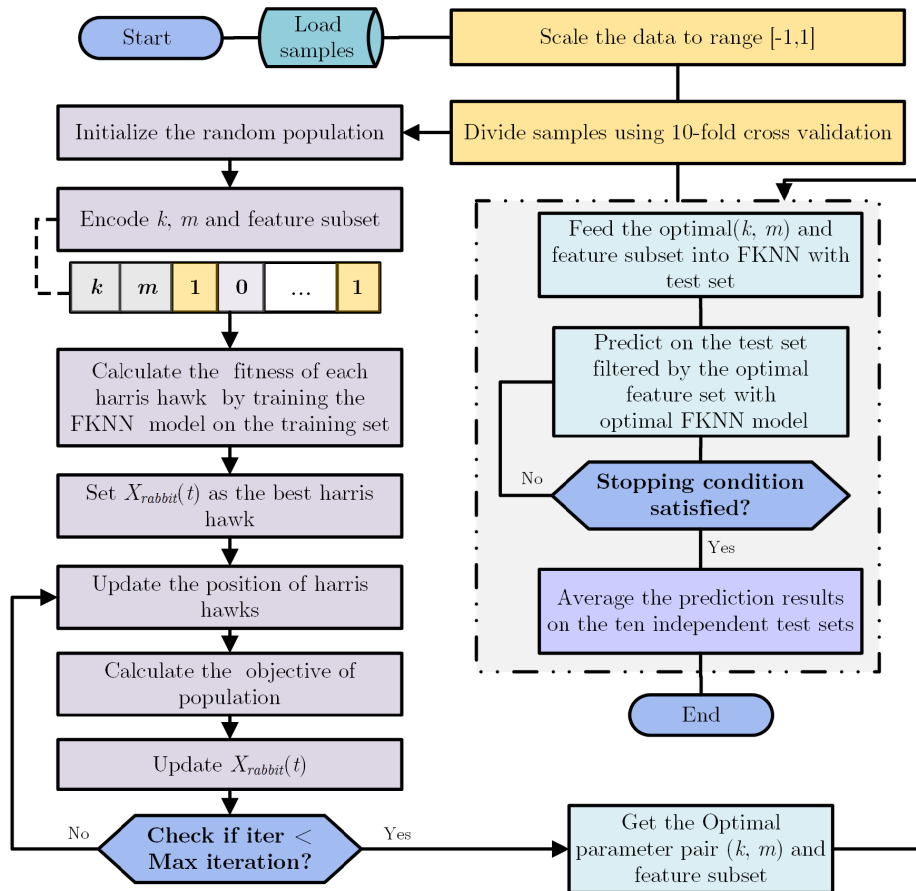


FIGURE 1. Flowchart of HHO-FKNN.

HHO-FKNN is substantiated for the first time to diagnose the severity of COVID-19. The active model is built using the info about patients’ necessary information, pre-existing diseases, symptoms, immune indexes, and complications. In the developed method (HHO-FKNN), HHO was employed to train an FKNN model and to explore the critical risk factors of COVID-19 infected people at the same time. In the experiment, HHO-FKNN is compared with the other machine learning methods like grey wolf optimizer (GWO)-based FKNN (GWO-FKNN), support vector machines (SVM), and random forest (RF). It is shown that the established HHO-FKNN method performs much better than its peers in terms of four evaluation metrics, including the classification accuracy (ACC), sensitivity, specificity, and Matthews Correlation Coefficients (MCC). Hence, the main contributions of this study can be listed as follows:

- (a) The well-established HHO was successfully applied to tackle the parameter tuning and feature selection for FKNN.
- (b) The proposed HHO-FKNN is employed for the diagnosis of the severity of COVID-19 for the first time.
- (c) It is the first time to diagnose the severity of COVID-19 based on an immune index.
- (d) The established HHO-FKNN model outperforms other evolutionary-based competitors.

The structure of this article is as bellow. Section 2 described the data and proposed the HHO-FKNN model in detail. The experimental arrangement and marks are explained in Section 3. Section 4 presents the discussions. The conclusions and upcoming works are presented in Section 5.

II. HHO-FKNN METHOD

The flowchart of HHO-FKNN is exposed in Figure 1. The whole procedure comprises data acquisition, standardization, feature selection, and classification. The first phase is to normalize the records, then using the HHO approach to select the informative features from the data samples and optimize the two critical parameters of the FKNN model. Then the FKNN classifier is trained again by using the optimal parameters and feature subset. Finally, the optimal FKNN classifier is taken to determine whether the specific patient is severe or non-severe. The commonly used 10-fold cross-validation (CV) scheme is used to divide the data and obtain more accurate and unbiased experimental results, often adopted by many studies [67]–[74].

A. PARAMETER OPTIMIZATION AND FEATURE SELECTION BY HHO

Healthcare and diagnosis systems have many hardware and software aspects considered and modeled [75], [76].

Any inaccuracy in the diagnosis can lead to a crisis [77]. This research focuses on developing a hybrid HHO-FKNN prediction core to be utilized for diagnostic purposes. In this model, the feature selection core utilizes a binary model of HHO. As we know, the primary method of HHO is a continuous approach verified on a set of problems with no binary variable. HHO was invented by Heidari *et al.* [78] as a new swarm-based algorithm for solving a set of unconstrained or even constrained cases. This method also has its exclusive features based on hawks and rabbits' greedy actions in wildlife [79]. This method found its widespread applications in dealing with different problems [80]–[82].

This research deals with a feature selection problem that inherits both continuous and binary optimization aspects. From the other side, we know the initial HHO is not compatible with binary spaces. However, we need to optimize both types of variables. Thus, we aim to advance the hybrid HHO by combining the continuous variant and the binary type to optimize any parameters.

B. CLASSIFICATION BASED ON FKNN

FKNN is used as a core prediction engine, which is used to perform classification tasks after obtaining the optimal parameters and feature subset. FKNN [83], [84] classifier is developed based on the traditional k-nearest neighbor (KNN) classifier and has been widely considered from the time when it was initially suggested [85], [86], [86]–[88]. Compared with procedures such as extreme learning machines [89]–[94], deep learning methods [95]–[97], and support vector machines [70], [17], [98]–[103], FKNN is much simpler and can return outcomes that can be more easily understood.

Up to now, FKNN presented its capacity as a unique aspect of neighbor classification and case-based learning [104]. It is one of the most significant characteristics of FKNN to represent inaccurate information and provide samples belonging to related categories. After being allocated a membership, we can classify each sample into a class with the highest membership value. Many works utilized FKNN because of its competitive advantages. For examples, it found its application in various scenarios, including slope collapse prediction scenarios [105], protein identification and prediction scenarios [106], [107], medical diagnosis cases [87], [108], bankruptcy prediction models [86], and grouting activity prediction scenarios [109]. Logically, there is no perfect model and method in the artificial intelligence area. For instance, FKNN suffers from some issues; one of them is its dependency on two key parameters, the fuzzy intensity factor (*m*) and the number of neighbors (*k*). Therefore, these two limits have to be adjusted correctly to attain a superior classification efficacy. In this research, we employed the HHO to adjust the parameters of FKNN.

To implement the fuzzy *k*-NN system, we follow the next operations:

Step 1: Consider

$$X_R = \{x_i\}_{i=1}^{m_R}$$

to be the reference set we have at hand and

$$W = \{w_i\}_{i=1}^{m_R}$$

be a set of *i*-dimensional vectors.

Step 2:

$$w_i = (w_{i,1}, w_{i,2}, \dots, w_{i,l}) \quad \sum_{j=1}^l w_{i,j} = 1 \text{ and } 0 \leq w_{i,j} \leq 1$$

For every $w_{i,j}$, $1 \leq i \leq m_R$, $1 \leq j \leq l$, and *l* denotes the number of classes.

Step 3: For each *x* that we want to classify, we can attain the set *K* of indices that correspond with the “*k* nearest neighbors of *x* in X_R and the fuzzy decision-vector” [83].

$$v = \left(\sum_{x \in K} w_s \right) / k$$

Step 4: If the user is involved in a non-fuzzy decision, ties are wrecked randomly or by the single NN law. If all $w_{i,j}$, $1 \leq i \leq m_R$, $1 \leq j \leq l$, are equivalent to 0 or 1, then we can consider the fuzzy *k*-NN instruction equivalents to the normal *k*-NN rule.

C. PROPOSED HHO-FKNN

To utilize and explore the potential of KNN, its parameters are optimized and adjusted using the HHO. It is also appointed to determine the optimal feature subsets in the datasets. Here, we describe the main steps of feature selection and parameter optimization of the proposed HHO-FKNN model:

Step 1: Load samples and scale the data.

Step 2: Divide samples using 10-fold cross-validation.

Step 3: Initialize the input parameters of HHO. These parameters are population, population size, bounds, space dimension, and numbers of iterations.

Step 4: Encode *k*, *m*, and feature subset.

Step 5: Cross-boundary treatment and calculation of population fitness.

Step 6: Update parameters *E*.

$$E = 2E_0 \left(1 - \frac{t}{T} \right) \tag{1}$$

where E_0 is a random number of $[-1, 1]$.

Step 7: Attain the fitness value with (*k*, *m*) and the chosen features for each swarm member referring to the following rule.

$$\begin{cases} f_1 = \frac{\sum_{i=1}^K acc_i}{K} \\ f_2 = 1 - \frac{\sum_{j=1}^n bin_j}{n} \\ f = \alpha \times f_1 + \beta \times f_2 \end{cases} \tag{2}$$

Here we determine the objective function needs to be minimized. The first sub-objective function f_1 denotes the average accuracy degree realized by the FKNN through K-fold CV, where $K = 5$ and acc_i denote the i th fold CV's accuracy. For another sub-objective rule (function) f_2 , bin_j shows the j th feature's binary value, and n denotes the full number of features. In the resulted objective formulation, which is shown using f , we have two scaling factors. One of them is α , which shows the weight of the accuracy term decided by the user. Simultaneously, the other, denoted by β , indicates the scale weighting for the selected features [110].

Step 8: Choose the first best hawk (solution) with extreme fitness value and keep them as $X_{rabbit}(t)$.

Step 9: Update the location according to the three main parts of "soft besiege," "hard besiege," and "soft besiege with rapid progressive divides." The updating rule that hawks follow to catch the rabbits during the "soft besiege" phase is as follow:

$$X(t+1) = \Delta X(t) - E |JX_{rabbit}(t) - X(t)| \quad (3)$$

$$\Delta X(t) = X_{rabbit}(t) - X(t) \quad (4)$$

where J is a random number of $[0, 2]$.

The updating equation of the "hard besiege" step is expressed as follows:

$$X(t+1) = X_{rabbit}(t) - E |\Delta X(t)| \quad (5)$$

The updated formula of "soft besiege with progressive rapid divides" is as follow:

$$Y = X_{rabbit}(t) - E |JX_{rabbit}(t) - X(t)| \quad (6)$$

$$Z = Y + S \times LF(D) \quad (7)$$

D is the case's dimension we want to solve, and S indicates a random vector by size $1 \times D$. LF is the call function of Levy's fight.

Step 10: Calculate the objective of the population.

Step 11: Go to step 3 if the maximum number of iterations has not been reached.

Step 12: Get the optimal parameter pair (k, m) and feature subset and Feed the optimal (k, m) and feature subset into FKNN with the test set.

Step 13: Go to step 12 if the condition is not satisfied.

Step 14: Average the prediction results on the ten independent test sets.

Step 15: Print and post-process the first two elements of $X_{rabbit}(t)$ as the optimal FKNN pair (k, m) and the other n dimensions of the binary values of $X_{rabbit}(t)$ as the indicators of the finest subset of the feature.

III. EXPERIMENTAL SETUP AND RESULTS

This section compares the proposed CPA with several conventional and recent optimizers in the field. All experiments

were conducted on Windows Server 2008 R2 operating system with Intel (R) Xeon (R) Silver 4110 CPU (2.10 GHz) (2.10GHz) and 128 GB of RAM. We coded all algorithms for comparison on the MATLAB R2014b.

A. DATA COLLECTION

A retrospective review of medical records was conducted for 47 patients with COVID-19 pneumonia admitted to the *Affiliated Yueqing Hospital of Wenzhou Medical University* (Yueqing, China) from Jan 21 to Mar 10, 2020. Severe acute respiratory syndrome coronavirus 2 (SARS-CoV-2) testing performed on admission on all patients with COVID-19 pneumonia using real-time reverse transcriptional polymerase chain reaction (RT-PCR). All patients were SARS-CoV-2-positive. The COVID-19 pneumonia was spotted referring to the New Coronavirus Pneumonia Prevention and Control Program published by the National Health Commission of the People's Republic of China in 2020 [111]. To simplify the data analysis, patients were categorized into two groups, severe ($n = 21$) and non-severe cases ($n = 26$). Patients were required to encounter at least one of the next criteria for the diagnosis of severe COVID-19:

- (i) Respiratory distress with respiratory frequency $\geq 30/\text{min}$;
- (ii) Resting oxygen saturation $\leq 93\%$;
- (iii) Oxygenation index (arterial oxygen pressure (PaO₂, mmHg)/fraction of inspired oxygen (FiO₂) ratios, PaO₂/FiO₂) ≤ 300 mmHg.

A detailed description of the utilized database for research is tabulated in Table 1. This study was permitted by the Ethics Committees of the *Affiliated Yueqing Hospital of Wenzhou Medical University* (code: 202000002) and complied with the Helsinki declaration. The clinical parameter and immunological indices were analyzed by an independent sample t-test, using SPSS version 21.0 (IBM, Somers, NY, USA). A p-value < 0.05 was considered to be statistically significant. Detailed results of the statistical analysis are described in Table 2.

Table 3 records the time relative values of one iteration of HHO-FKNN and GWO-FKNN. In the table, the relative value of HHO-FKNN running time is set as 1, and 1.07 is the running time of GWO-FKNN relative to HHO-FKNN. The larger the value is, the longer the running time.

B. EXPERIMENTAL SETUP

In this section, we need to run a set of experiments to substantiate the HHO-based model's efficacy in diagnosing the COVID-19. The investigated methods, comprising HHO-FKNN and GWO-FKNN [112], were realized from scratch based on the software of MATLAB. We normalized the input data to be inside $[-1, 1]$ in advance of the classification's performance. The stratified 10-fold CV was employed with our tests to weigh the value of the classification results (costs) and guarantee not having biased results. The maximum iterations and the number of members in the swarm

TABLE 1. Description of 31 attributes.

| No. | Feature | Detailed description |
|-----|--------------------------------|---|
| F1 | Gender | Male = 0; Female= 1 |
| F2 | Age | Severe cases (mean, standard deviation) =61.43±17.64 Non-severe cases (mean, standard deviation) = 42.58±11.62 |
| F3 | CD4 T-lymphocyte count (CD4 T) | Severe cases (mean, standard deviation) =313.67±164.53 Non-severe cases (mean, standard deviation) = 719.00±238.63 |
| F4 | CD8 T-lymphocyte count (CD8 T) | Severe cases (mean, standard deviation) =184.09±118.34 Non-severe cases (mean, standard deviation) = 464.36±143.39 |
| F5 | Contact history (CH) | Wuhan Sojourn=1; Hubei Sojourn=2; Wuhan patient contact=3; Hubei patient contact=4; Other regions patient contact=5; No contact=6 |
| F6 | Smoking history (SH) | No = 0; Yes = 1 |
| F7 | Drinking history (DH) | No = 0; Yes = 1 |
| F8 | Hypertension (HP) | No = 0; Yes = 1 |
| F9 | Diabetes mellitus (DM) | No = 0; Yes = 1 |
| F10 | Chronic kidney disease (CKD) | No = 0; Yes = 1 |
| F11 | Chronic liver disease (CLD) | No = 0; Yes = 1 |
| F12 | Chronic heart disease (CHD) | No = 0; Yes = 1 |
| F13 | Chronic lung disease (CLGD) | No = 0; Yes = 1 |
| F14 | Malignant tumor (MT) | No = 0; Yes = 1 |
| F15 | Fever | No = 0; Yes = 1 |
| F16 | Cough | No = 0; Yes = 1 |
| F17 | Sputum | No = 0; Yes = 1 |
| F18 | Nasal obstruction (NO) | No = 0; Yes = 1 |
| F19 | Sore throat (ST) | No = 0; Yes = 1 |
| F20 | Fatigue | No = 0; Yes = 1 |
| F21 | Myalgia | No = 0; Yes = 1 |
| F22 | Headache | No = 0; Yes = 1 |
| F23 | Nausea/Vomiting (N/V) | No = 0; Yes = 1 |
| F24 | Abdominal Pain (AP) | No = 0; Yes = 1 |
| F25 | Diarrhea | No = 0; Yes = 1 |
| F26 | Shock | No = 0; Yes = 1 |
| F27 | Vasopressor drug (VD) | No = 0; Yes = 1 |
| F28 | Acute kidney injury (AKI) | No = 0; Yes = 1 |
| F29 | Acute myocardial injury (AMI) | No = 0; Yes = 1 |
| F30 | Acute liver injury (ALI) | No = 0; Yes = 1 |
| F31 | Secondary infection (SI) | No = 0; Yes = 1 |

TABLE 2. Immunological & clinical parameter in severe patients and non-severe patients.

| Index | Severe (n = 21) | Non-severe (n = 26) | p-value |
|-------------|-----------------|---------------------|---------|
| Age (years) | 61.43±17.64 | 42.58±11.62 | 0.000 |
| CD4 T (μl) | 313.67±164.53 | 719.00±238.63 | 0.000 |
| CD8 T (μl) | 184.09±118.34 | 464.36±143.39 | 0.000 |

were set at 50 and 20, respectively. The searching variety for the two strictures in FKNN is determined as follows

The involved methods, HHO-FKNN and GWO-FKNN [112] were both implemented from scratch in the MAT-

TABLE 3. Comparison of CPU running time between HHO-FKNN and GWO-FKNN.

| Algorithm | Relative running time | Ranking |
|-----------|-----------------------|---------|
| HHO-FKNN | 1 | 1 |
| GWO-FKNN | 1.07 | 2 |

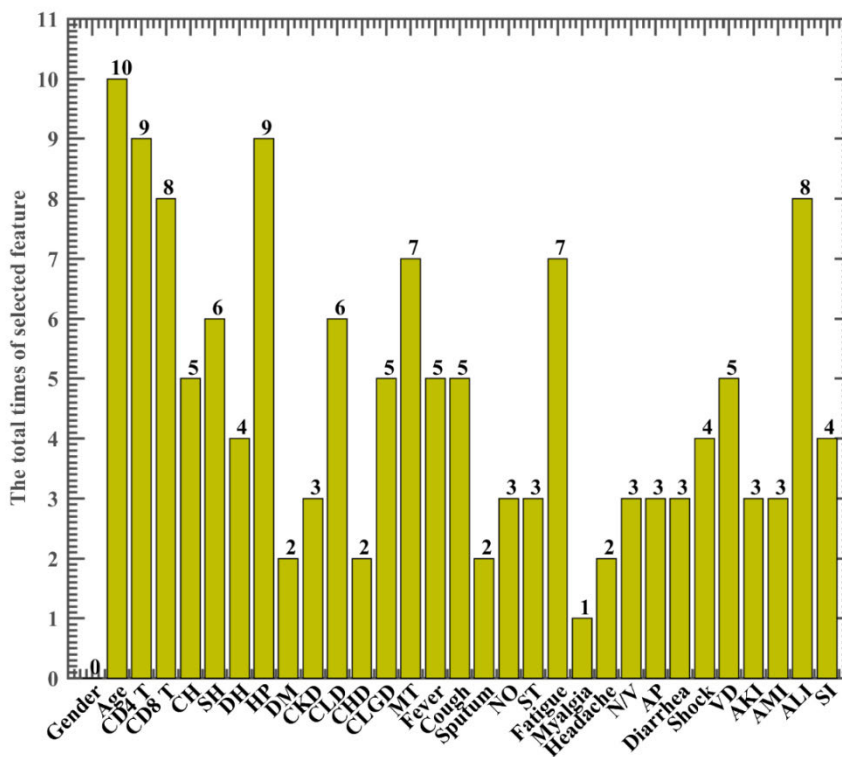


FIGURE 2. Frequency of the features obtained by HHO-FKNN via the 10-fold CV.

LAB environment. We have respected fair comparisons referring to the neural network literature [113]–[115]. There is no biased test due to advantageous testing conditions [116]–[120]. Before we perform the classification, we normalize the data into the range $[-1, 1]$. Also, we employed a 10-fold cross-validation CV for evaluating the efficacies to ensure unbiased results. There should be a limit for the time of execution, which is set to 50 iterations. Also, we require that each method starts with 20 agents inside the feature space. For searching ranges of dual factors in FKNN, we have $k \in [1, 5]$, $m \in [1, 5]$. LIBSVM and RF tools³ were used to run SVM and RF models.

C. EXPERIMENTAL RESULTS

To assess the HHO-FKNN with the feature selection (FS) method, we utilized well-regarded criteria such as classification accuracy (ACC), sensitivity, specificity, and Matthews’s correlation coefficient (MCC). Table 4 shows the four

³ <https://www.csie.ntu.edu.tw/~cjlin/libsvm/>, and <https://code.google.com/archive/p/randomforest-matlab>.

evaluation indicators’ specific values, including classification accuracy, MCC, sensitivity, specificity, and shows the results of four evaluation indicators using the mean and variance. The means of the four evaluation indicators of the model are 94.00%, 0.8891, 90.00%, and 96.67%, and their variances are 0.0966, 0.1791, 0.2108, and 0.1054, respectively. Also, according to the experimental results, it is obvious that the HHO algorithm can automatically obtain the optimal parameters of FKNN and provides the optimal feature subset at the same time.

The frequency of each feature selected by HHO-FKNN via a 10-fold CV procedure is illustrated in Figure 2. As shown, As shown, Age, CD4 T, HP, CD8 T, ALI, and Fatigue are the five features with the highest frequency, and they seem 10, 9, 9, 8, 8, and 7 times, respectively. It means they contain the most discriminative information for recognizing the severe patients and non-severe patients. Therefore, these five informative factors need to be focused on clinically.

To validate the technique’s success, it is compared with six other operational machine learning models, including HHO-FKNN without FS, GWO-FKNN with FS, and

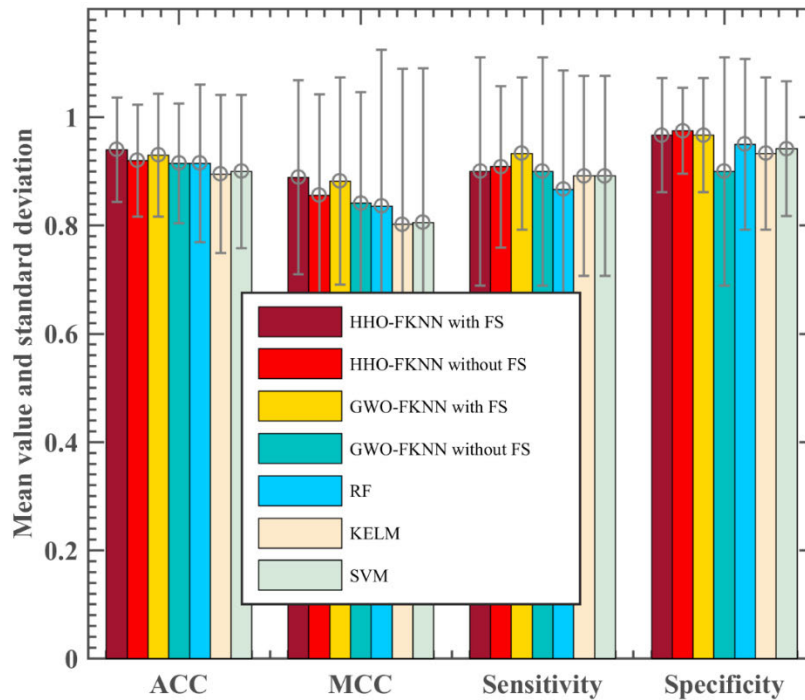


FIGURE 3. Classification efficacy of seven models based on the ACC, MCC, sensitivity, and specificity.

TABLE 4. Classification performance of HHO-FKNN in terms of ACC, MCC, sensitivity, and specificity.

| Fold | Optimal features | ACC | MCC | Sensitivity | Specificity |
|-------|---|--------|--------|-------------|-------------|
| No.1 | {F2, F3, F4, F5, F8, F11, F13, F14, F16, F19, F20, F24, F26, F27, F31} | 1.0000 | 1.0000 | 1.0000 | 1.0000 |
| No.2 | {F2, F3, F4, F6, F8, F10, F11, F14, F15, F16, F17, F19, F20, F27, F30, F31} | 0.8000 | 0.6124 | 0.5000 | 1.0000 |
| No.3 | {F2, F3, F4, F5, F6, F7, F8, F9, F13, F16, F22, F23, F28, F29, F30, F31} | 1.0000 | 1.0000 | 1.0000 | 1.0000 |
| No.4 | {F2, F3, F4, F5, F6, F7, F8, F10, F14, F15, F20, F29, F30} | 1.0000 | 1.0000 | 1.0000 | 1.0000 |
| No.5 | {F2, F3, F4, F5, F6, F8, F13, F17, F18, F20, F22, F24, F25, F27, F30} | 1.0000 | 1.0000 | 1.0000 | 1.0000 |
| No.6 | {F2, F4, F8, F11, F14, F15, F18, F20, F23, F27, F30} | 1.0000 | 1.0000 | 1.0000 | 1.0000 |
| No.7 | {F2, F3, F5, F6, F7, F8, F11, F12, F13, F14, F20, F25, F26, F28, F30} | 0.8000 | 0.6124 | 0.5000 | 1.0000 |
| No.8 | {F2, F3, F4, F6, F7, F8, F9, F11, F13, F15, F16, F18, F20, F24, F26, F31} | 1.0000 | 1.0000 | 1.0000 | 1.0000 |
| No.9 | {F2, F3, F8, F10, F12, F14, F21, F23, F26, F30} | 1.0000 | 1.0000 | 1.0000 | 1.0000 |
| No.10 | {F2, F3, F4, F11, F14, F15, F16, F19, F25, F27, F28, F29, F30} | 1.0000 | 1.0000 | 1.0000 | 1.0000 |
| AVG. | - | 0.9400 | 0.8891 | 0.9000 | 0.9667 |
| STD | - | 0.0966 | 0.1791 | 0.2108 | 0.1054 |

GWO-FKNN without FS, RF, KELM, and SVM. According to the comparison results shown in Figure 3, the HHO-FKNN with the FS model is superior to the HHO-FKNN without the FS model in both the classification accuracy rate and the Matthews correlation coefficient. Its variance on these two indicators is also less than that of the HHO-FKNN without FS model. However, in terms of sensitivity and specificity, the HHO-FKNN with the FS model is inferior to the HHO-FKNN without the FS model. Its variance on these two indicators is also more significant than that of the HHO-FKNN without the FS model. Therefore, it is evident that the HHO-FKNN with the FS model with the feature selection algorithm has a better accuracy. The following are HHO-FKNN without FS, GWO-FKNN without FS, RF, SVM, and KELM. Besides, the accuracy of RF and

GWO-FKNN without FS is the same HHO-FKNN with FS is two percentage points higher than HHO-FKNN without FS, and the variance of KELM is the largest, reaching 0.1462. In terms of the MCC evaluation index, HHO-FKNN with the FS model still achieved the best results, followed by GWO-FKNN with FS, which was 0.7 percentage points lower than HHO-FKNN with FS, HHO-FKNN without FS ranked third, which was 3.33 percentage points lower than HHO-FKNN with FS. Followed by GWO-FKNN without FS, RF, SVM, and KELM, KELM, and SVM are not much different; HHO-FKNN with FS has the smallest variance, and RF variance is the largest, reaching 0.2893. In terms of sensitivity evaluation index, GWO-FKNN with FS model has the best evaluation effect, followed HHO-FKNN without FS model has only 2.5 percentage points difference with

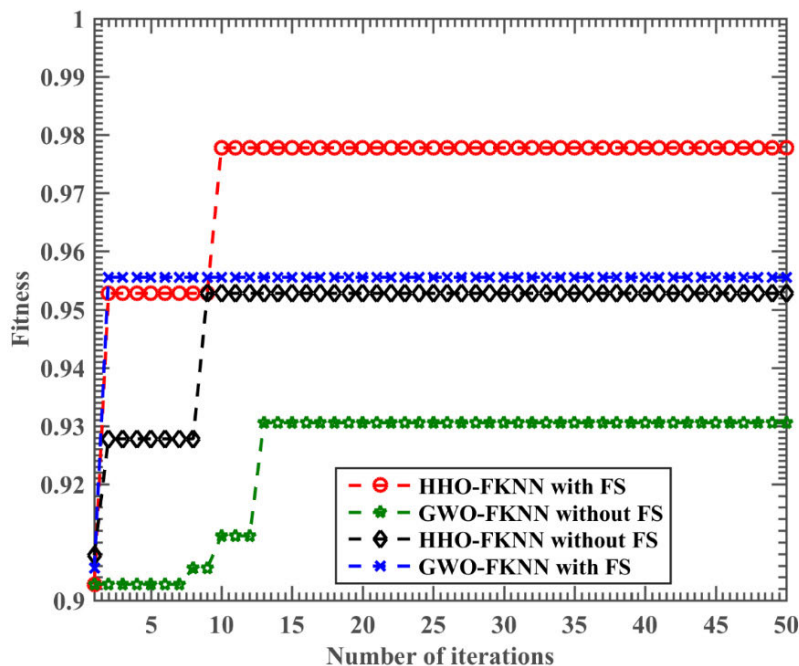


FIGURE 4. Relationship between training accuracy of HHO-FKNN with FS, HHO-FKNN without FS, GWO-FKNN with FS, and GWO-FKNN without FS and the number of iterations.

it, HHO-FKNN with FS and GWO-FKNN without FS is the same, HHO-FKNN with FS model is 0.83 percentage points lower than HHO-FKNN without FS model. Finally, the values of KELM and SVM are the same, the variance of GWO-FKNN with FS is the lowest, and the variance of RF is the largest, reaching 0.2194. In terms of specific evaluation indexes, HHO-FKNN without the FS model has the best results and the smallest variance, followed by GWO-FKNN with FS and HHO-FKNN with FS are the same. They are 0.83 percentage points lower than HHO-FKNN without FS. The next models are RF, SVM, and KELM. The worst is GWO-FKNN without FS, which is only 90.00%. GWO-FKNN without FS has the most considerable variance, reaching 0.2108.

In terms of these specific evaluation indexes, HHO-FKNN without the FS model has the best results and the smallest variance, followed by GWO-FKNN with FS and HHO-FKNN with FS are the same. Their values are both 0.83 percentage points lower than HHO-FKNN without FS. The next models are RF, SVM, and KELM. The worst is GWO-FKNN without FS, which is only 90.00%. GWO-FKNN without FS has the most considerable variance, reaching 0.2108. As per the results observed in Figure 4, we observe that the HHO-FKNN with the FS model can speedily and unceasingly jump out of local minima, which leads to better accuracy rates. This also indicates the HHO-FKNN with the FS method makes a delicate balance between exploratory and exploitative leanings.

The new framework takes advantage of the dynamic and time-varying operations of HHO when shifting from

exploratory drifts to intensification tendencies. Compared to other methods such as GWO, there is no highly focused intensification in HHO, which may result in immature convergence. Generally speaking, when HHO can smoothly shift from its initial exploration to the four stages of its exploitation, it shows a high local optima avoidance rate. Besides, there is a levy flight pattern within HHO’s search phases, which helps this method scan the explored parameters’ vicinity accurately. Then, after determining potential weights, it can enhance the quality of them using its greedy operation. Due to these reasons, we observed a very satisfactory performance within the parameter optimization and feature selection phases. By further observing the curve in Figure 4, it was found that the HHO-FKNN without the FS model is liable to fall into a local optimum, and the accuracy is not as high as that of HHO-FKNN with FS. Although the GWO-FKNN with the FS model ranks second in accuracy, it tends to fall into a local optimum in the late search period. Among all algorithms, GWO-FKNN without FS has the lowest accuracy that is much smaller than that of the GWO-FKNN with the FS model. With continuous iteration, its accuracy improvement is not apparent, and it is easy to fall into a local optimum.

IV. DISCUSSIONS

HHO-FKNN machine learning model has been established for clear discrimination between severe and non-severe patients and identified several critical indicators, including advanced age, Hypertension, acute liver injury, and CD4 T cells, CD8 T cells, and fatigue. The results were consistent with previous research. Furthermore, HHO-FKNN can help

determine the severity of the COVID-19 patients' condition quickly and help inform clinical decision-making.

Research studies conducted based on SARS and Middle East Respiratory Syndrome (MERS) infection identified advanced age as a critical factor in determining recovery [121]–[123]. It has been reported that compared with younger macaques inoculated with SARS-CoV, older macaques showed a more robust host antiviral response, which is positively related to inflammation-related genes and type I interferon [124]. Additionally, accumulating evidence shows that the incidence of severe infection and severe sepsis increased with advanced age [125], [126]. It has been generally believed that age-dependent defects in T- and B-lymphocyte function could contribute to increased risk of infection, and over-secretion of type 2 cytokines may stimulate enhanced viral replication [127]–[129]. Taken together, advanced age has adverse impacts on disease recovery.

We are also alarmed about whether patients with cardiovascular illness are at bigger risk for COVID-19. A large population-based study from Canada reported that more than 600 Middle East Respiratory Syndrome Coronavirus (MERS-CoV) cases suggested that hypertension and diabetes mellitus are prevalent in about 50% of the severe cases [130]. Hypertension was an independent predictor of many diseases, including acute coronary syndrome, acute ischaemic stroke, and recurrent colorectal adenoma [131]–[133]. However, the literature on the effects of Hypertension on SARS, MERS, and COVID-19 is scarce. With the spread of COVID-19 and an increase in the number of cases, mortality was higher among COVID-19 infected individuals with comorbidities such as Hypertension, diabetes mellitus, coronary heart disease, cerebral infarction, and chronic lung disease [134]. For example, Chen and colleagues found that in 99 COVID-19 cases, forty percent of patients had cardiovascular and cerebrovascular diseases [135]. Huang *et al.* reported that 20% of COVID-19 patients have diabetes mellitus [134]. In line with these findings, Li *et al.* also revealed that the proportion of COVID-19 patients with Hypertension was two-fold higher in severe cases compared to non-severe cases [136]. Thus, these findings demonstrate that chronic cardiovascular comorbidities with COVID-19 patients were more likely to have a poor prognosis.

A high incidence of acute liver injury (ALI) in SARS patients has been reported (up to 60%). Also, it has been reported in patients infected with MERS-CoV [137], [138]. Several clinical observations have suggested that liver impairment commonly occurs in patients with COVID-19 [135], [139], [140]. These data show that hepatic comorbidities complicated 2–11 % of COVID-19 patients. Elevated serum levels of alanine aminotransferase (ALT) and aspartate aminotransferase (AST) have been reported in 14–53% of COVID-19 cases. ALT and AST are the most frequently used parameters of liver function. A study with many patients from multiple centers in China suggested that compared to the non-severe patients, ALT and AST levels were significantly increased in the severe patients [141]. In a study of

intensive care unit (ICU) patients, it was shown that AST levels increased significantly in patients with ICU compared with non-severe patients [2]. Huang and colleagues revealed that the pathological Liver profile of COVID-19 patients, including moderate microvascular steatosis and mild lobular and portal activity, might have been attributable to SARS-CoV-2 infection. These findings demonstrate a relationship between liver impairment and COVID-19, which plays a critical role in disease progression and is associated with risks of COVID-19 [142].

Lymphocytes are critical immune cells divided into three subsets: T lymphocytes, B lymphocytes, and natural killer (NK) cells [143]. Lymphocytes are a kind of white blood cell that plays a pivotal role in adaptive immune function and is a central component of the immune system [144]. The immune response can recognize and remember antigens to eliminate invading bacteria, viruses and so on. Zhou *et al.* reported that CD4 T cells could reflect the body's immune function. The lower level of the CD4 T cells indicates that the patient immune function level is low [145]. COVID-19 and SARS-CoV belong to coronavirus, and the genomic sequence similarity between COVID-19 and SARS-CoV is very high [146]. For instance, He and colleagues demonstrated that the CD4 T cells, CD8 T cells in peripheral blood were decreased significantly in SARS coronavirus-infected individuals lymphocyte counts may aid with predicting the severity and clinical outcomes [147]. Therefore, similar to SARS coronaviruses, we speculate that COVID-19 may also destroy the immune system, resulting in T lymphocyte immune deficiency. However, the mechanism of the reduction of peripheral blood lymphocytes in patients with COVID-19 is not precise.

However, this research's findings should be interpreted with thoughtfulness and carefulness due to several potential limitations that we faced during this research. First, this research's sample size is limited; thus, further research is required to improve diagnostic accuracy. It is scheduled that the HHO-FKNN can be further improved and optimized using a large number of patients from multiple centers. Second, in this study, we focused our investigation only on severe and non-severe patients. Future studies need to focus on discriminating more types of COVID-19. Third, the features of COVID-19 involved, though, are likely to be limited. We recommend the inclusion of more metrics of COVID-19 status such as blood routine, blood biochemistry, arterial blood gas analysis, coagulation function, and systemic inflammatory markers in future studies.

V. CONCLUSION AND FUTURE WORKS

Based on patients' necessary information, pre-existing diseases, symptom, immune index, and complication, this study established a useful HHO-FKNN model to distinguish the severity of COVID-19, of which innovations are as follows: on the one hand, it is proposed for the first time to use the immune index to distinguish the severity of COVID-19, and on the other hand, the HHO algorithm is used for the first

time to screen the parameters and features of the FKNN simultaneously. According to the experimental results, the proposed method shows higher prediction accuracy and more stable performance than other machine learning algorithms on the COVID-19 severity prediction problem to select the key factors with more discriminating ability simultaneously. For future work, we will first try to apply the proposed HHO-FKNN to the COVID-19 pre-diagnosis problem and then try to apply it to solve other infectious disease prediction problems.

For future work, the proposed HHO can be wrapped with other popular learning methods such as extreme learning machines [72], [73], [90], [148]–[150], support vector machines [151]–[155], and convolutional neural networks [95], [156]–[158] for the COVID-19 diagnosis task. Furthermore, the improved version of HHO can be developed on some other real fields like video coding optimization [159], feature information fusion [160], social evolution modeling [161], recommender system [162], text clustering [163], unsupervised band selection [164], which are also exciting topics that worthy of the investigation soon.

ACKNOWLEDGMENT

This research will be supported by an online web service for any query at <https://aliasgharheidari.com>. (Hua Ye, Peiliang Wu, and Tianru Zhu are co-first authors.)

REFERENCES

- [1] N. Zhu, D. Zhang, W. Wang, X. Li, B. Yang, J. Song, X. Zhao, B. Huang, W. Shi, R. Lu, P. Niu, F. Zhan, X. Ma, D. Wang, W. Xu, G. Wu, G. F. Gao, D. Phil, W. Tan, and P. Niu, "A novel coronavirus from patients with pneumonia in China, 2019," *New Eng. J. Med.*, vol. 382, no. 8, pp. 727–733, Feb. 2020.
- [2] C. Huang, Y. Wang, X. Li, L. Ren, J. Zhao, Y. Hu, and L. Zhang, "Clinical features of patients infected with 2019 novel coronavirus in Wuhan, China," *Lancet*, vol. 395, pp. 497–506, May 2020.
- [3] L. C. S. Afonso, G. H. Rosa, C. R. Pereira, S. A. T. Weber, C. Hook, V. H. C. Albuquerque, and J. P. Papa, "A recurrence plot-based approach for Parkinson's disease identification," *Future Gener. Comput. Syst.*, vol. 94, pp. 282–292, May 2019.
- [4] F. Zhou, T. Yu, R. Du, G. Fan, Y. Liu, Z. Liu, J. Xiang, Y. Wang, B. Song, X. Gu, L. Guan, Y. Wei, H. Li, X. Wu, J. Xu, S. Tu, Y. Zhang, H. Chen, and B. Cao, "Clinical course and risk factors for mortality of adult inpatients with COVID-19 in wuhan, China: A retrospective cohort study," *Lancet*, vol. 395, no. 10229, pp. 1054–1062, Mar. 2020.
- [5] Q. Ruan, K. Yang, W. Wang, L. Jiang, and J. Song, "Clinical predictors of mortality due to COVID-19 based on an analysis of data of 150 patients from wuhan, China," *Intensive Care Med.*, vol. 46, no. 5, pp. 846–848, Mar. 2020.
- [6] Y. Liu, Y. Yang, C. Zhang, and F. Huang, F. Wang, "Clinical and biochemical indexes from 2019-nCoV infected patients linked to viral loads and lung injury," *Sci. China Life Sci.*, vol. 63, no. 3, pp. 364–374, Mar. 2020.
- [7] E. Y. Li, C.-Y. Tung, and S.-H. Chang, "The wisdom of crowds in action: Forecasting epidemic diseases with a Web-based prediction market system," *Int. J. Med. Informat.*, vol. 92, pp. 35–43, Aug. 2016.
- [8] N. Kimura, Y. Aso, K. Yabuuchi, M. Ishibashi, D. Hori, Y. Sasaki, A. Nakamichi, S. Uesugi, H. Fujioka, S. Iwao, M. Jikumaru, T. Katayama, K. Sumi, A. Eguchi, S. Nonaka, M. Kakumu, and E. Matsubara, "Modifiable lifestyle factors and cognitive function in older people: A cross-sectional observational study," *Frontiers Neurol.*, vol. 10, p. 401, Apr. 2019.
- [9] Z. Obermeyer and E. J. Emanuel, "Predicting the future—Big data, machine learning, and clinical medicine," *New England J. Med.*, vol. 375, p. 1216, Sep. 29 2016.
- [10] B. Cao, W. Dong, Z. Lv, Y. Gu, S. Singh, and P. Kumar, "Hybrid microgrid many-objective sizing optimization with fuzzy decision," *IEEE Trans. Fuzzy Syst.*, vol. 28, no. 11, pp. 2702–2710, Nov. 2020.
- [11] B. Cao, X. Wang, W. Zhang, H. Song, and Z. Lv, "A many-objective optimization model of industrial Internet of Things based on private blockchain," *IEEE Network*, vol. 34, no. 5, pp. 78–83, Sep./Oct. 2020.
- [12] X. Fu, P. Pace, G. Aloï, L. Yang, and G. Fortino, "Topology optimization against cascading failures on wireless sensor networks using a memetic algorithm," *Comput. Netw.*, vol. 177, Aug. 2020, Art. no. 107327.
- [13] S. Qu, Y. Han, Z. Wu, and H. Raza, "Consensus modeling with asymmetric cost based on data-driven robust optimization," *Group Decis. Negotiation*, vol. 4, pp. 1–38, Sep. 2020.
- [14] B. Cao, J. Zhao, P. Yang, Y. Gu, K. Muhammad, J. J. P. C. Rodrigues, and V. H. C. de Albuquerque, "Multiobjective 3-D topology optimization of next-generation wireless data center network," *IEEE Trans. Ind. Informat.*, vol. 16, no. 5, pp. 3597–3605, May 2020.
- [15] B. Cao, J. Zhao, Y. Gu, Y. Ling, and X. Ma, "Applying graph-based differential grouping for multiobjective large-scale optimization," *Swarm Evol. Comput.*, vol. 53, Mar. 2020, Art. no. 100626.
- [16] B. Cao, S. Fan, J. Zhao, P. Yang, K. Muhammad, and M. Tanveer, "Quantum-enhanced multiobjective large-scale optimization via parallelism," *Swarm Evol. Comput.*, vol. 57, Sep. 2020, Art. no. 100697.
- [17] H. Huang, X. Feng, S. Zhou, J. Jiang, H. Chen, Y. Li, and C. Li, "A new fruit fly optimization algorithm enhanced support vector machine for diagnosis of breast cancer based on high-level features," *BMC Bioinf.*, vol. 20, no. S8, p. 290, Jun. 2019.
- [18] A. A. Mousavi, C. Zhang, S. F. Masri, and G. Gholipour, "Structural damage localization and quantification based on a CEEMDAN Hilbert transform neural network approach: A model steel truss bridge case study," *Sensors*, vol. 20, no. 5, p. 1271, Feb. 2020.
- [19] Y. Chen, L. He, Y. Guan, H. Lu, and J. Li, "Life cycle assessment of greenhouse gas emissions and water-energy optimization for shale gas supply chain planning based on multi-level approach: Case study in barnett, marcellus, fayetteville, and haynesville shales," *Energy Convers. Manage.*, vol. 134, pp. 382–398, Feb. 2017.
- [20] B. Wang, B. Zhang, X. Liu, and F. Zou, "Novel infrared image enhancement optimization algorithm combined with DFOCS," *Optik*, vol. 224, Dec. 2020, Art. no. 165476.
- [21] C. Wu, P. Wu, J. Wang, R. Jiang, M. Chen, and X. Wang, "Critical review of data-driven decision-making in bridge operation and maintenance," *Struct. Infrastruct. Eng.*, vol. 5, pp. 1–24, Nov. 2020.
- [22] S. Liu, W. Yu, F. T. S. Chan, and B. Niu, "A variable weight-based hybrid approach for multi-attribute group decision making under interval-valued intuitionistic fuzzy sets," *Int. J. Intell. Syst.*, vol. 36, pp. 1015–1052, Nov. 2020.
- [23] S. Liu, F. T. S. Chan, and W. Ran, "Decision making for the selection of cloud vendor: An improved approach under group decision-making with integrated weights and objective/subjective attributes," *Expert Syst. Appl.*, vol. 55, pp. 37–47, Aug. 2016.
- [24] C. Cai, X. Gao, Q. Teng, R. Kiran, J. Liu, Q. Wei, and Y. Shi, "Hot isostatic pressing of a near α -Ti alloy: Temperature optimization, microstructural evolution and mechanical performance evaluation," *Mater. Sci. Eng., A*, Oct. 2020, Art. no. 140426.
- [25] B. Cao, J. Zhao, Y. Gu, S. Fan, and P. Yang, "Security-aware industrial wireless sensor network deployment optimization," *IEEE Trans. Ind. Informat.*, vol. 16, no. 8, pp. 5309–5316, Aug. 2020.
- [26] E. Liu, W. Li, H. Cai, and S. Peng, "Formation mechanism of trailing oil in product oil pipeline," *Processes*, vol. 7, no. 1, p. 7, Dec. 2018.
- [27] J. Guo, X. Zhang, F. Gu, H. Zhang, and Y. Fan, "Does air pollution stimulate electric vehicle sales? Empirical evidence from twenty major cities in China," *J. Cleaner Prod.*, vol. 249, Mar. 2020, Art. no. 119372.
- [28] B. Zhu, B. Su, and Y. Li, "Input-output and structural decomposition analysis of India's carbon emissions and intensity, 2007/08–2013/14," *Appl. Energy*, vol. 230, pp. 1545–1556, Nov. 2018.
- [29] C.-W. Zhang, J.-P. Ou, and J.-Q. Zhang, "Parameter optimization and analysis of a vehicle suspension system controlled by magnetorheological fluid dampers," *Struct. Control Health Monitor.*, vol. 13, no. 5, pp. 885–896, 2006.
- [30] J. Yan, W. Pu, S. Zhou, H. Liu, and M. S. Greco, "Optimal resource allocation for asynchronous multiple targets tracking in heterogeneous radar networks," *IEEE Trans. Signal Process.*, vol. 68, pp. 4055–4068, 2020.
- [31] T. Qiu, X. Shi, J. Wang, Y. Li, S. Qu, Q. Cheng, T. Cui, and S. Sui, "Deep learning: A rapid and efficient route to automatic metasurface design," *Adv. Sci.*, vol. 6, no. 12, Jun. 2019, Art. no. 1900128.

- [32] T. Li, M. Xu, C. Zhu, R. Yang, Z. Wang, and Z. Guan, "A deep learning approach for multi-frame in-loop filter of HEVC," *IEEE Trans. Image Process.*, vol. 28, no. 11, pp. 5663–5678, Nov. 2019.
- [33] H. Chen, A. Chen, L. Xu, H. Xie, H. Qiao, Q. Lin, and K. Cai, "A deep learning CNN architecture applied in smart near-infrared analysis of water pollution for agricultural irrigation resources," *Agricult. Water Manage.*, vol. 240, Oct. 2020, Art. no. 106303.
- [34] C. Cai, X. Wu, W. Liu, W. Zhu, H. Chen, J. C. D. Qiu, C.-N. Sun, J. Liu, Q. Wei, and Y. Shi, "Selective laser melting of near- α titanium alloy Ti-6Al-2Zr-1Mo-1 V: Parameter optimization, heat treatment and mechanical performance," *J. Mater. Sci. Technol.*, vol. 57, pp. 51–64, Nov. 2020.
- [35] R. Pang, B. Xu, X. Kong, and D. Zou, "Seismic fragility for high CFRDs based on deformation and damage index through incremental dynamic analysis," *Soil Dyn. Earthq. Eng.*, vol. 104, pp. 432–436, Jan. 2018.
- [36] Z. Xiong, N. Xiao, F. Xu, X. Zhang, Q. Xu, K. Zhang, and C. Ye, "An equivalent exchange based data forwarding incentive scheme for socially aware networks," *J. Signal Process. Syst.*, vol. 2, pp. 1–15, Nov. 2020.
- [37] J. Yan, W. Pu, S. Zhou, H. Liu, and Z. Bao, "Collaborative detection and power allocation framework for target tracking in multiple radar system," *Inf. Fusion*, vol. 55, pp. 173–183, Mar. 2020.
- [38] H. Yue, H. Wang, H. Chen, K. Cai, and Y. Jin, "Automatic detection of feather defects using lie group and fuzzy Fisher criterion for shuttlecock production," *Mech. Syst. Signal Process.*, vol. 141, Jul. 2020, Art. no. 106690.
- [39] Z. Lv and N. Kumar, "Software defined solutions for sensors in 6G/loE," *Comput. Commun.*, vol. 153, pp. 42–47, Mar. 2020.
- [40] S. Song, P. Wang, A. A. Heidari, M. Wang, X. Zhao, H. Chen, W. He, and S. Xu, "Dimension decided harris hawks optimization with Gaussian mutation: Balance analysis and diversity patterns," *Knowl.-Based Syst.*, vol. 5, Oct. 2020, Art. no. 106425, doi: [10.1016/j.knsys.2020.106425](https://doi.org/10.1016/j.knsys.2020.106425).
- [41] D. Zhao, L. Liu, F. Yu, A. A. Heidari, M. Wang, D. Oliva, K. Muhammad, and H. Chen, "Ant colony optimization with horizontal and vertical crossover search: Fundamental visions for multi-threshold image segmentation," *Expert Syst. Appl.*, vol. 4, Oct. 2020, Art. no. 114122, doi: [10.1016/j.eswa.2020.114122](https://doi.org/10.1016/j.eswa.2020.114122).
- [42] X. Zhang, Y. Xu, C. Yu, A. A. Heidari, S. Li, H. Chen, and C. Li, "Gaussian mutational chaotic fruit fly-built optimization and feature selection," *Expert Syst. Appl.*, vol. 141, Mar. 2020, Art. no. 112976.
- [43] X. Wang, H. Chen, A. A. Heidari, X. Zhang, J. Xu, Y. Xu, and H. Huang, "Multi-population following behavior-driven fruit fly optimization: A Markov chain convergence proof and comprehensive analysis," *Knowl.-Based Syst.*, vol. 210, Art. no. 106437, Sep. 2020, doi: [10.1016/j.knsys.2020.106437](https://doi.org/10.1016/j.knsys.2020.106437).
- [44] D. Zhao, L. Liu, F. Yu, A. A. Heidari, M. Wang, G. Liang, K. Muhammad, and H. Chen, "Chaotic random spare ant colony optimization for multi-threshold image segmentation of 2D kapur entropy," *Knowl.-Based Syst.*, Oct. 2020, Art. no. 106510.
- [45] J. Tu, H. Chen, J. Liu, A. A. Heidari, X. Zhang, M. Wang, R. Ruby, and Q.-V. Pham, "Evolutionary biogeography-based whale optimization methods with communication structure: Towards measuring the balance," *Knowl.-Based Syst.*, vol. 212, Jan. 2021, Art. no. 106642.
- [46] H. Chen, D. L. Fan, L. Fang, W. Huang, J. Huang, C. Cao, L. Yang, Y. He, and L. Zeng, "Particle swarm optimization algorithm with mutation operator for particle filter noise reduction in mechanical fault diagnosis," *Int. J. Pattern Recognit. Artif. Intell.*, vol. 34, no. 10, Sep. 2020, Art. no. 2058012.
- [47] L. Yang and H. Chen, "Fault diagnosis of gearbox based on RBF-PF and particle swarm optimization wavelet neural network," *Neural Comput. Appl.*, vol. 31, no. 9, pp. 4463–4478, Sep. 2019.
- [48] Y. Cao, Y. Li, G. Zhang, K. Jermittiparsert, and M. Nasser, "An efficient terminal voltage control for PEMFC based on an improved version of whale optimization algorithm," *Energy Rep.*, vol. 6, pp. 530–542, Nov. 2020.
- [49] J. Liu, C. Wu, G. Wu, and X. Wang, "A novel differential search algorithm and applications for structure design," *Appl. Math. Comput.*, vol. 268, pp. 246–269, Oct. 2015.
- [50] G. Sun, B. Yang, Z. Yang, and G. Xu, "An adaptive differential evolution with combined strategy for global numerical optimization," *Soft Comput.*, vol. 15, pp. 1–20, Mar. 2019.
- [51] S. Li, H. Chen, M. Wang, A. A. Heidari, and S. Mirjalili, "Slime mould algorithm: A new method for stochastic optimization," *Future Gener. Comput. Syst.*, vol. 111, pp. 300–323, Oct. 2020.
- [52] G. G. Wang, S. Deb, and Z. Cui, "Monarch butterfly optimization," *Neural Comput. Appl.*, vol. 31, no. 7, pp. 1995–2014, 2019.
- [53] G.-G. Wang, "Moth search algorithm: A bio-inspired Metaheuristic algorithm for global optimization problems," *Memetic Comput.*, vol. 10, no. 2, pp. 151–164, Jun. 2018.
- [54] H. Chen, A. A. Heidari, H. Chen, M. Wang, Z. Pan, and A. H. Gandomi, "Multi-population differential evolution-assisted Harris hawks optimization: Framework and case studies," *Future Gener. Comput. Syst.*, vol. 111, pp. 175–198, Oct. 2020.
- [55] Y. Zhang, R. Liu, X. Wang, H. Chen, and C. Li, "Boosted binary Harris hawks optimizer and feature selection," *Eng. Comput.*, vol. 25, p. 26, May 2020, doi: [10.1007/s00366-020-01028-5](https://doi.org/10.1007/s00366-020-01028-5).
- [56] S. Jiao, G. Chong, C. Huang, H. Hu, M. Wang, A. A. Heidari, H. Chen, and X. Zhao, "Orthogonally adapted harris hawks optimization for parameter estimation of photovoltaic models," *Energy*, vol. 203, Jul. 2020, Art. no. 117804.
- [57] M. A. Al-Betar, M. A. Awadallah, A. A. Heidari, H. Chen, H. Al-khraisat, and C. Li, "Survival exploration strategies for harris hawks optimizer," *Expert Syst. Appl.*, vol. 7, Nov. 2020, Art. no. 114243, doi: [10.1016/j.eswa.2020.114243](https://doi.org/10.1016/j.eswa.2020.114243).
- [58] M. A. Elaziz, A. A. Heidari, H. Fujita, and H. Moayedi, "A competitive chain-based harris hawks optimizer for global optimization and multi-level image thresholding problems," *Appl. Soft Comput.*, vol. 95, Oct. 2020, Art. no. 106347.
- [59] S. Gupta, K. Deep, A. A. Heidari, H. Moayedi, and M. Wang, "Opposition-based learning Harris hawks optimization with advanced transition rules: Principles and analysis," *Expert Syst. Appl.*, vol. 158, Nov. 2020, Art. no. 113510.
- [60] K. Shao, W. Fu, J. Tan, and K. Wang, "Coordinated approach fusing time-shift multiscale dispersion entropy and vibrational Harris hawks optimization-based SVM for fault diagnosis of rolling bearing," *Measurement*, vol. 10, Oct. 2020, Art. no. 108580.
- [61] Y. Tikhamarine, D. Souag-Gamane, A. N. Ahmed, S. S. Sammen, O. Kisi, Y. F. Huang, and A. El-Shafie, "Rainfall-runoff modelling using improved machine learning methods: Harris hawks optimizer vs. Particle swarm optimization," *J. Hydrol.*, vol. 589, Oct. 2020, Art. no. 125133.
- [62] B. Abbasi, T. Babaei, Z. Hosseini, K. Smith-Miles, and M. Dehghani, "Predicting solutions of large-scale optimization problems via machine learning: A case study in blood supply chain management," *Comput. Oper. Res.*, vol. 119, Jul. 2020, Art. no. 104941.
- [63] I. S. Amiri, P. Yupaipin, B. Mahapatra, S. K. Tripathy, and G. Palai, "Computation of PUG concentration in human blood using the combination of photonics and machine learning," *Optik*, vol. 192, Sep. 2019, Art. no. 162968.
- [64] H. Ayyaz and S. Arslan Tuncer, "Determination of the effect of red blood cell parameters in the discrimination of iron deficiency anemia and beta thalassemia via neighborhood component analysis feature selection-based machine learning," *Chemometric Intell. Lab. Syst.*, vol. 196, Jan. 2020, Art. no. 103886.
- [65] A. Banerjee, S. Ray, B. Vorselaars, J. Kitson, M. Mamalakis, S. Weeks, M. Baker, and L. S. Mackenzie, "Use of machine learning and artificial intelligence to predict SARS-CoV-2 infection from full blood counts in a population," *Int. Immunopharmacol.*, vol. 86, Sep. 2020, Art. no. 106705.
- [66] D. Rammurthy and P. K. Mahesh, "Whale harris hawks optimization based deep learning classifier for brain tumor detection using MRI images," *J. King Saud Univ. Comput. Inf. Sci.*, Aug. 2020.
- [67] A. Lin, Q. Wu, A. A. Heidari, Y. Xu, H. Chen, W. Geng, Y. Li, and C. Li, "Predicting intentions of students for master programs using a chaos-induced sine cosine-based fuzzy K-Nearest neighbor classifier," *IEEE Access*, vol. 7, pp. 67235–67248, 2019.
- [68] G. Liu, W. Jia, M. Wang, A. A. Heidari, H. Chen, Y. Luo, and C. Li, "Predicting cervical hyperextension injury: A covariance guided sine cosine support vector machine," *IEEE Access*, vol. 8, pp. 46895–46908, 2020.
- [69] W. Zhu, C. Ma, X. Zhao, M. Wang, A. A. Heidari, H. Chen, and C. Li, "Evaluation of sino foreign cooperative education project using orthogonal sine cosine optimized kernel extreme learning machine," *IEEE Access*, vol. 8, pp. 61107–61123, 2020.
- [70] L. Shen, H. Chen, Z. Yu, W. Kang, B. Zhang, H. Li, B. Yang, and D. Liu, "Evolving support vector machines using fruit fly optimization for medical data classification," *Knowl.-Based Syst.*, vol. 96, pp. 61–75, Mar. 2016.

- [71] C. Li, L. Hou, B. Y. Sharma, H. Li, C. Chen, Y. Li, X. Zhao, H. Huang, Z. Cai, and H. Chen, "Developing a new intelligent system for the diagnosis of tuberculous pleural effusion," *Comput. Methods Programs Biomed.*, vol. 153, pp. 211–225, Jan. 2018.
- [72] J. Xia, H. Chen, Q. Li, M. Zhou, L. Chen, Z. Cai, Y. Fang, and H. Zhou, "Ultrasound-based differentiation of malignant and benign thyroid nodules: An extreme learning machine approach," *Comput. Methods Programs Biomed.*, vol. 147, pp. 37–49, Aug. 2017.
- [73] H.-L. Chen, G. Wang, C. Ma, Z.-N. Cai, W.-B. Liu, and S.-J. Wang, "An efficient hybrid kernel extreme learning machine approach for early diagnosis of Parkinson's disease," *Neurocomputing*, vol. 184, pp. 131–144, Apr. 2016.
- [74] M. Wang, H. Chen, B. Yang, X. Zhao, L. Hu, Z. Cai, H. Huang, and C. Tong, "Toward an optimal kernel extreme learning machine using a chaotic moth-flame optimization strategy with applications in medical diagnoses," *Neurocomputing*, vol. 267, pp. 69–84, Dec. 2017.
- [75] D. Wen, X. Zhang, X. Liu, and J. Lei, "Evaluating the consistency of current mainstream wearable devices in health monitoring: A comparison under free-living conditions," *J. Med. Internet Res.*, vol. 19, no. 3, p. e68, Mar. 2017.
- [76] J. Xie, D. Wen, L. Liang, Y. Jia, L. Gao, and J. Lei, "Evaluating the validity of current mainstream wearable devices in fitness tracking under various physical activities: Comparative study," *JMIR Health Health*, vol. 6, no. 4, p. e94, Apr. 2018.
- [77] Z. Lv and L. Qiao, "Analysis of healthcare big data," *Future Gener. Comput. Syst.*, vol. 109, pp. 103–110, Aug. 2020.
- [78] A. A. Heidari, S. Mirjalili, H. Faris, I. Aljarah, M. Mafarja, and H. Chen, "Harris hawks optimization: Algorithm and applications," *Future Gener. Comput. Syst.*, vol. 97, pp. 849–872, Aug. 2019.
- [79] J. C. Bednarz, "Cooperative hunting Harris' hawks (Parabuteo unicinctus)," *Science*, vol. 239, no. 4847, pp. 1525–1527, Mar. 1988.
- [80] H. Chen, S. Jiao, M. Wang, A. A. Heidari, and X. Zhao, "Parameters identification of photovoltaic cells and modules using diversification-enriched Harris hawks optimization with chaotic drifts," *J. Cleaner Prod.*, vol. 244, Jan. 2020, Art. no. 118778.
- [81] H. M. Ridha, A. A. Heidari, M. Wang, and H. Chen, "Boosted mutation-based Harris hawks optimizer for parameters identification of single-diode solar cell models," *Energy Convers. Manage.*, vol. 209, Apr. 2020, Art. no. 112660.
- [82] Y. Wei, H. Lv, M. Chen, M. Wang, A. A. Heidari, H. Chen, and C. Li, "Predicting entrepreneurial intention of students: An extreme learning machine with Gaussian barebone Harris hawks optimizer," *IEEE Access*, vol. 8, pp. 76841–76855, 2020.
- [83] A. Jówik, "A learning scheme for a fuzzy K-NN rule," *Pattern Recognit. Lett.*, vol. 1, nos. 5–6, pp. 287–289, Jul. 1983.
- [84] J. M. Keller, M. R. Gray, and J. A. Givens, "A fuzzy K-nearest neighbor algorithm," *IEEE Trans. Syst., Man, Cybern.*, vols. SMC-15, no. 4, pp. 580–585, Aug. 1985.
- [85] Z. Cai, J. Gu, C. Wen, D. Zhao, C. Huang, H. Huang, C. Tong, J. Li, and H. Chen, "An intelligent Parkinson's disease diagnostic system based on a chaotic bacterial foraging optimization enhanced fuzzy KNN approach," *Comput. Math. Methods Med.*, vol. 2018, pp. 1–24, Jun. 2018.
- [86] H.-L. Chen, B. Yang, G. Wang, J. Liu, X. Xu, S.-J. Wang, and D.-Y. Liu, "A novel bankruptcy prediction model based on an adaptive fuzzy k-nearest neighbor method," *Knowl.-Based Syst.*, vol. 24, no. 8, pp. 1348–1359, Dec. 2011.
- [87] H.-L. Chen, C.-C. Huang, X.-G. Yu, X. Xu, X. Sun, G. Wang, and S.-J. Wang, "An efficient diagnosis system for detection of Parkinson's disease using fuzzy k-nearest neighbor approach," *Expert Syst. Appl.*, vol. 40, no. 1, pp. 263–271, Jan. 2013.
- [88] W.-L. Zuo, Z.-Y. Wang, T. Liu, and H.-L. Chen, "Effective detection of Parkinson's disease using an adaptive fuzzy k-nearest neighbor approach," *Biomed. Signal Process. Control*, vol. 8, no. 4, pp. 364–373, Jul. 2013.
- [89] D. Zhao, C. Huang, Y. Wei, F. Yu, M. Wang, and H. Chen, "An effective computational model for bankruptcy prediction using kernel extreme learning machine approach," *Comput. Econ.*, vol. 49, no. 2, pp. 325–341, Feb. 2017.
- [90] H. Chen, Q. Zhang, J. Luo, Y. Xu, and X. Zhang, "An enhanced bacterial foraging optimization and its application for training kernel extreme learning machine," *Appl. Soft Comput.*, vol. 86, Jan. 2020, Art. no. 105884.
- [91] M. Wang, H. Chen, H. Li, Z. Cai, X. Zhao, C. Tong, J. Li, and X. Xu, "Grey wolf optimization evolving kernel extreme learning machine: Application to bankruptcy prediction," *Eng. Appl. Artif. Intell.*, vol. 63, pp. 54–68, Aug. 2017.
- [92] Q. Li, H. Chen, H. Huang, X. Zhao, Z. Cai, C. Tong, W. Liu, and X. Tian, "An enhanced grey wolf optimization based feature selection wrapped kernel extreme learning machine for medical diagnosis," *Comput. Math. Methods Med.*, vol. 2017, pp. 1–15, Dec. 2017.
- [93] T. Liu, L. Hu, C. Ma, Z.-Y. Wang, and H.-L. Chen, "A fast approach for detection of erythematous diseases based on extreme learning machine with maximum relevance minimum redundancy feature selection," *Int. J. Syst. Sci.*, vol. 46, no. 5, pp. 919–931, Apr. 2015.
- [94] H. Chen, B. Yang, D. Liu, W. Liu, Y. Liu, X. Zhang, and L. Hu, "Using blood indexes to predict overweight statuses: An extreme learning machine-based approach," *PLoS ONE*, vol. 10, no. 11, Nov. 2015, Art. no. e0143003.
- [95] Y. Li, W.-G. Cui, H. Huang, Y.-Z. Guo, K. Li, and T. Tan, "Epileptic seizure detection in EEG signals using sparse multiscale radial basis function networks and the Fisher vector approach," *Knowl.-Based Syst.*, vol. 164, pp. 96–106, Jan. 2019.
- [96] Y. Li, Y. Liu, W.-G. Cui, Y.-Z. Guo, H. Huang, and Z.-Y. Hu, "Epileptic seizure detection in EEG signals using a unified temporal-spectral Squeeze-and-Excitation network," *IEEE Trans. Neural Syst. Rehabil. Eng.*, vol. 28, no. 4, pp. 782–794, Apr. 2020, doi: 10.1109/TNSRE.2020.2973434.
- [97] J. Li, Y. Wang, J. See, and W. Liu, "Micro-expression recognition based on 3D flow convolutional neural network," *Pattern Anal. Appl.*, vol. 22, no. 4, pp. 1331–1339, Nov. 2019.
- [98] H. L. Chen, B. Yang, S. J. Wang, G. Wang, D. Y. Liu, H. Z. Li, and W. B. Liu, "Towards an optimal support vector machine classifier using a parallel particle swarm optimization strategy," *Appl. Math. Comput.*, vol. 239, pp. 180–197, Jul. 2014.
- [99] M. Wang and H. Chen, "Chaotic multi-swarm whale optimizer boosted support vector machine for medical diagnosis," *Appl. Soft Comput.*, vol. 88, Mar. 2020, Art. no. 105946.
- [100] H. Chen, S. Li, A. Asghar Heidari, P. Wang, J. Li, Y. Yang, M. Wang, and C. Huang, "Efficient multi-population outpost fruit fly-driven optimizers: Framework and advances in support vector machines," *Expert Syst. Appl.*, vol. 142, Mar. 2020, Art. no. 112999.
- [101] Y. Wang, J. See, Y.-H. Oh, R. C.-W. Phan, Y. Rahulamathavan, H.-C. Ling, S.-W. Tan, and X. Li, "Effective recognition of facial micro-expressions with video motion magnification," *Multimedia Tools Appl.*, vol. 76, no. 20, pp. 21665–21690, Oct. 2017.
- [102] D. Wang, H. Qiao, B. Zhang, and M. Wang, "Online support vector machine based on convex hull vertices selection," *IEEE Trans. Neural Netw. Learn. Syst.*, vol. 24, no. 4, pp. 593–609, Apr. 2013.
- [103] Q. Zhang, D. Wang, and Y. Wang, "Convergence of decomposition methods for support vector machines," *Neurocomputing*, vol. 317, pp. 179–187, Nov. 2018.
- [104] J. Derrac, S. García, and F. Herrera, "Fuzzy nearest neighbor algorithms: Taxonomy, experimental analysis and prospects," *Inf. Sci.*, vol. 260, pp. 98–119, Mar. 2014.
- [105] M.-Y. Cheng and N.-D. Hoang, "A swarm-optimized fuzzy instance-based learning approach for predicting slope collapses in mountain roads," *Knowl.-Based Syst.*, vol. 76, pp. 256–263, Mar. 2015.
- [106] Y. Huang and Y. Li, "Prediction of protein subcellular locations using fuzzy k-NN method," *Bioinformatics*, vol. 20, no. 1, pp. 21–28, Jan. 2004.
- [107] J. Sim, S.-Y. Kim, and J. Lee, "Prediction of protein solvent accessibility using fuzzy k-nearest neighbor method," *Bioinformatics*, vol. 21, no. 12, pp. 2844–2849, Jun. 2005.
- [108] D. Y. Liu, H. L. Chen, B. Yang, X. E. Lv, L. N. Li, and J. Liu, "Design of an enhanced fuzzy k-nearest neighbor classifier based computer aided diagnostic system for thyroid disease," *J. Med. Syst.*, vol. 36, pp. 3243–3254, Oct. 2012.
- [109] M.-Y. Cheng and N.-D. Hoang, "Groutability estimation of grouting processes with microfine cements using an evolutionary instance-based learning approach," *J. Comput. Civil Eng.*, vol. 28, no. 4, Jul. 2014, Art. no. 04014014.
- [110] L. Hu, H. Li, Z. Cai, F. Lin, G. Hong, H. Chen, and Z. Lu, "A new machine-learning method to prognosticate paraquat poisoned patients by combining coagulation, liver, and kidney indices," *PLoS ONE*, vol. 12, no. 10, Oct. 2017, Art. no. e0186427.

- [111] S. Khan, L. Peng, R. Siddique, G. Nabi, and M. Xue, "Impact of COVID-19 infection on pregnancy outcomes and the risk of maternal-to-neonatal intrapartum transmission of COVID-19 during natural birth," *Infection Control Hospital Epidemiol.*, vol. 41, no. 6, pp. 748–750, 2020.
- [112] J. Zhu, F. Zhu, S. Huang, G. Wang, H. Chen, X. Zhao, and S.-Y. Zhang, "A new evolutionary machine learning approach for identifying pyrene induced hepatotoxicity and renal dysfunction in rats," *IEEE Access*, vol. 7, pp. 15320–15329, 2019.
- [113] K. Shi, J. Wang, Y. Tang, and S. Zhong, "Reliable asynchronous sampled-data filtering of T-S fuzzy uncertain delayed neural networks with stochastic switched topologies," *Fuzzy Sets Syst.*, vol. 381, pp. 1–25, Feb. 2020.
- [114] K. Shi, J. Wang, S. Zhong, Y. Tang, and J. Cheng, "Non-fragile memory filtering of T-S fuzzy delayed neural networks based on switched fuzzy sampled-data control," *Fuzzy Sets Syst.*, vol. 394, pp. 40–64, Sep. 2020.
- [115] K. Shi, Y. Tang, S. Zhong, C. Yin, X. Huang, and W. Wang, "Nonfragile asynchronous control for uncertain chaotic lurie network systems with Bernoulli stochastic process," *Int. J. Robust Nonlinear Control*, vol. 28, no. 5, pp. 1693–1714, Mar. 2018.
- [116] S. Yang, B. Deng, J. Wang, H. Li, M. Lu, Y. Che, X. Wei, and K. A. Loparo, "Scalable digital neuromorphic architecture for large-scale biophysically meaningful neural network with multi-compartment neurons," *IEEE Trans. Neural Netw. Learn. Syst.*, vol. 31, no. 1, pp. 148–162, Jan. 2020.
- [117] H. Zhang, Z. Wang, W. Chen, A. A. Heidari, M. Wang, X. Zhao, G. Liang, H. Chen, and X. Zhang, "Ensemble mutation-driven salp swarm algorithm with restart mechanism: Framework and fundamental analysis," *Expert Syst. Appl.*, vol. 165, Mar. 2021, Art. no. 113897.
- [118] T. Ni, H. Chang, T. Song, Q. Xu, Z. Huang, H. Liang, A. Yan, and X. Wen, "Non-intrusive online distributed pulse shrinking-based interconnect testing in 2.5D IC," *IEEE Trans. Circuits Syst. II, Exp. Briefs*, vol. 67, no. 11, pp. 2657–2661, Nov. 2020.
- [119] H. Zhang, Z. Qiu, J. Cao, M. Abdel-Aty, and L. Xiong, "Event-triggered synchronization for neutral-type semi-Markovian neural networks with partial mode-dependent time-varying delays," *IEEE Trans. Neural Netw. Learn. Syst.*, vol. 31, no. 11, pp. 4437–4450, Nov. 2020.
- [120] Z. Lv and L. Qiao, "Deep belief network and linear perceptron based cognitive computing for collaborative robots," *Appl. Soft Comput.*, vol. 92, Jul. 2020, Art. no. 106300.
- [121] M. S. Majumder, S. A. Klumberg, S. R. Mekaru, and J. S. Brownstein, "Mortality risk factors for middle east respiratory syndrome outbreak, South Korea, 2015," *Emerg Infect Dis.*, vol. 21, p. 2088, Nov. 2015.
- [122] K. Hong, J. Choi, S. Hong, J. Lee, J. Kwon, and S. Kim, "Predictors of mortality in Middle East respiratory syndrome (MERS)," *Thorax*, vol. 73, pp. 286–289, Mar. 2018.
- [123] K. Choi, T. Chau, O. Tsang, and E. Tso, "Outcomes and prognostic factors in 267 patients with severe acute respiratory syndrome in Hong Kong," *Ann. Internal Med.*, vol. 139, pp. 715–723, Nov. 2003.
- [124] S. L. Smits, A. de Lang, J. M. A. van den Brand, L. M. Leijten, W. F. van Icken, M. J. C. Eijkemans, G. van Amerongen, T. Kuiken, A. C. Andeweg, A. D. M. E. Osterhaus, and B. L. Haagmans, "Exacerbated innate host response to SARS-CoV in aged non-human primates," *PLoS Pathogens*, vol. 6, no. 2, Feb. 2010, Art. no. e1000756.
- [125] D. Pittet, B. Thievent, R. P. Wenzel, N. Li, G. Gurman, and P. M. Suter, "Importance of pre-existing co-morbidities for prognosis of septicemia in critically ill patients," *Intensive Care Med.*, vol. 19, pp. 265–272, 1993.
- [126] G. S. Martin, D. M. Mannino, S. Eaton, and M. Moss, "The epidemiology of sepsis in the United States from 1979 through 2000," *New England J. Med.*, vol. 348, pp. 1546–1554, Apr. 17 2003.
- [127] M. E. Weksler, "Changes in the B-cell repertoire with age," *Vaccine*, vol. 18, no. 16, pp. 1624–1628, Feb. 2000.
- [128] D. Weiskopf, B. Weinberger, and B. Grubeck-Loebenstein, "The aging of the immune system," *Transpl Int.*, vol. 22, pp. 1041–1050, Nov. 2009.
- [129] S. M. Opal, T. D. Girard, and E. W. Ely, "The immunopathogenesis of sepsis in elderly patients," *Clin. Infectious Diseases*, vol. 41, no. 7, pp. S504–S512, Nov. 2005.
- [130] A. Badawi and S. G. Ryoo, "Prevalence of comorbidities in the middle east respiratory syndrome coronavirus (MERS-CoV): A systematic review and meta-analysis," *Int. J. Infectious Diseases*, vol. 49, pp. 33–129, Aug. 2016.
- [131] G. Ntaios, O. Gurer, M. Faouzi, C. Aubert, and P. Michel, "Hypertension is an independent predictor of mean platelet, vol. in, patients with acute ischaemic stroke," *Int. Med. J.*, vol. 41, pp. 691–695, Sep. 2011.
- [132] S. Najjar, A. Scuteri, V. Shetty, and J. Wright, "Pulse wave velocity is an independent predictor of the longitudinal increase in systolic blood pressure and of incident hypertension in the Baltimore Longitudinal Study of Aging," *J. Amer. College Cardiol.*, vol. 51, pp. 1377–1383, Apr. 2008.
- [133] J. Ge, J. Li, H. Yu, and B. Hou, "Hypertension is an independent predictor of multivessel coronary artery disease in young adults with acute coronary syndrome," *Int. J. Hypertens.*, vol. 2018, Dec. 2018, Art. no. 7623639.
- [134] S.-Q. Deng and H.-J. Peng, "Characteristics of and public health responses to the coronavirus disease 2019 outbreak in China," *J. Clin. Med.*, vol. 9, no. 2, p. 575, Feb. 2020.
- [135] N. Chen, M. Zhou, X. Dong, J. Qu, F. Gong, Y. Han, Y. Qiu, J. Wang, Y. Liu, Y. Wei, J. Xia, T. Yu, X. Zhang, and L. Zhang, "Epidemiological and clinical characteristics of 99 cases of 2019 novel coronavirus pneumonia in wuhan, China: A descriptive study," *Lancet*, vol. 395, no. 10223, pp. 507–513, Feb. 2020.
- [136] B. Li, J. Yang, F. Zhao, L. Zhi, X. Wang, L. Liu, and Z. Bi, "Prevalence and impact of cardiovascular metabolic diseases on COVID-19 in China," *Clin. Res. Cardiol.*, vol. 109, pp. 531–538, Mar. 2020.
- [137] T. Chau, K. Lee, H. Yao, T. Tsang, and T. Chow, "SARS-associated viral hepatitis caused by a novel coronavirus: Report of three cases," *Hepatology*, vol. 39, pp. 302–310, Feb. 2004.
- [138] K. O. Alsaad, A. H. Hajeer, M. Al Balwi, M. Al Moaiqel, N. Al Oudah, A. Al Ajlan, S. AlJohani, S. Alsolamy, G. E. Gmati, H. Balkhy, H. H. Al-Jahdali, S. A. Baharoon, and Y. M. Arabi, "Histopathology of middle east respiratory syndrome coronavirus (MERS-CoV) infection—clinicopathological and ultrastructural study," *Histopathology*, vol. 72, no. 3, pp. 516–524, Feb. 2018.
- [139] D. Wang, B. Hu, C. Hu, F. Zhu, X. Liu, J. Zhang, B. Wang, H. Xiang, Z. Cheng, Y. Xiong, Y. Zhao, Y. Li, X. Wang, and Z. Peng, "Clinical characteristics of 138 hospitalized patients with 2019 novel coronavirus-infected pneumonia in Wuhan, China," *JAMA*, vol. 323, no. 11, p. 1061, Mar. 2020.
- [140] H. Shi, X. Han, N. Jiang, Y. Cao, O. Alwalid, J. Gu, Y. Fan, and C. Zheng, "Radiological findings from 81 patients with COVID-19 pneumonia in wuhan, China: A descriptive study," *Lancet Infectious Diseases*, vol. 20, no. 4, pp. 425–434, Apr. 2020.
- [141] W. Guan, Z. Ni, Y. Hu, W. Liang, C. Ou, J. He, and L. Liu, "Clinical characteristics of coronavirus disease 2019 in China," *New England J. Med.*, vol. 382, pp. 1708–1720, Apr. 2020.
- [142] Z. Xu, L. Shi, Y. Wang, J. Zhang, L. Huang, C. Zhang, S. Liu, P. Zhao, H. Liu, L. Zhu, Y. Tai, C. Bai, T. Gao, J. Song, P. Xia, J. Dong, J. Zhao, and F.-S. Wang, "Pathological findings of COVID-19 associated with acute respiratory distress syndrome," *Lancet Respiratory Med.*, vol. 8, no. 4, pp. 420–422, Apr. 2020.
- [143] Y. Okada, T. Hirota, Y. Kamatani, and A. Takahashi, "Identification of nine novel loci associated with white blood cell subtypes in a Japanese population," *PLoS Genet.*, vol. 7, no. 6, Jun. 2011, Art. no. e1002067.
- [144] N. K. Badr El-Din, S. M. Abdel Fattah, D. Pan, L. Tolentino, and M. Ghoneum, "Chemopreventive activity of MGN-3/Biobran against chemical induction of glandular stomach carcinogenesis in rats and its apoptotic effect in gastric cancer cells," *Integrative Cancer Therapies*, vol. 15, no. 4, pp. NP26–NP34, Dec. 2016.
- [145] E. Beswick, J. Johnson, and J. Saada, "TLR4 activation enhances the PD-L1-mediated tolerogenic capacity of colonic CD90+ stromal cells," *J. Immunol.*, vol. 193, pp. 2218–2229, Sep. 2014.
- [146] D. Benvenuto, M. Giovanetti, A. Ciccozzi, S. Spoto, S. Angeletti, and M. Ciccozzi, "The 2019-new coronavirus epidemic: Evidence for virus evolution," *J. Med. Virol.*, vol. 92, pp. 455–459, Apr. 2020.
- [147] Z. He, C. Zhao, Q. Dong, H. Zhuang, and S. Song, "Effects of severe acute respiratory syndrome (SARS) coronavirus infection on peripheral blood lymphocytes and their subsets," *Int. J. Infectious Diseases*, vol. 9, pp. 323–330, Nov. 2005.
- [148] L. Hu, G. Hong, J. Ma, X. Wang, and H. Chen, "An efficient machine learning approach for diagnosis of paraquat-poisoned patients," *Comput. Biol. Med.*, vol. 59, pp. 116–124, Apr. 2015.
- [149] L. Hu, P. Yang, X. Wang, F. Lin, H. Chen, H. Cao, and H. Li, "Using biochemical indexes to prognose paraquat-poisoned patients: An extreme learning machine-based approach," *IEEE Access*, vol. 7, pp. 42148–42155, 2019.
- [150] H. Zhao, H. Liu, J. Xu, and W. Deng, "Performance prediction using high-order differential mathematical morphology gradient spectrum entropy and extreme learning machine," *IEEE Trans. Instrum. Meas.*, vol. 69, no. 7, pp. 4165–4172, Jul. 2020, doi: [10.1109/TIM.2019.2948414](https://doi.org/10.1109/TIM.2019.2948414).

- [151] H. Chen, L. Hu, H. Li, G. Hong, T. Zhang, J. Ma, and Z. Lu, "An effective machine learning approach for prognosis of paraquat poisoning patients using blood routine indexes," *Basic Clin. Pharmacol. Toxicol.*, vol. 120, no. 1, pp. 86–96, Jan. 2017.
- [152] J. Tu, A. Lin, H. Chen, Y. Li, and C. Li, "Predict the entrepreneurial intention of fresh graduate students based on an adaptive support vector machine framework," *Math. Problems Eng.*, vol. 2019, pp. 1–16, Jan. 2019.
- [153] Y. Wei, N. Ni, D. Liu, H. Chen, M. Wang, and Q. Li, "An improved grey wolf optimization strategy enhanced SVM and its application in predicting the second major," *Math. Problems Eng.*, vol. 2017, Feb. 2017, Art. no. 9316713, doi: [10.1155/2017/9316713](https://doi.org/10.1155/2017/9316713).
- [154] L. Hu, F. Lin, H. Li, C. Tong, Z. Pan, J. Li, and H. Chen, "An intelligent prognostic system for analyzing patients with paraquat poisoning using arterial blood gas indexes," *J. Pharmacol. Toxicol. Methods*, vol. 84, pp. 78–85, Mar. 2017.
- [155] Z. Cai, J. Gu, and H.-L. Chen, "A new hybrid intelligent framework for predicting Parkinson's disease," *IEEE Access*, vol. 5, pp. 17188–17200, 2017.
- [156] X. Zhang, T. Wang, J. Wang, G. Tang, and L. Zhao, "Pyramid channel-based feature attention network for image dehazing," *Comput. Vis. Image Understand.*, vols. 197–198, Aug. 2020, Art. no. 103003, doi: [10.1016/j.cviu.2020.103003](https://doi.org/10.1016/j.cviu.2020.103003).
- [157] Y. Li, J. Liu, Z. Tang, and B. Lei, "Deep spatial-temporal feature fusion from adaptive dynamic functional connectivity for MCI identification," *IEEE Trans. Med. Imag.*, vol. 39, no. 9, pp. 2818–2830, Sep. 2020.
- [158] W. Deng, H. Liu, J. Xu, H. Zhao, and Y. Song, "An improved quantum-inspired differential evolution algorithm for deep belief network," *IEEE Trans. Instrum. Meas.*, vol. 69, no. 10, pp. 7319–7327, Oct. 2020, doi: [10.1109/TIM.2020.2983233](https://doi.org/10.1109/TIM.2020.2983233).
- [159] Y. Zhou, L. Tian, C. Zhu, X. Jin, and Y. Sun, "Video coding optimization for virtual reality 360-degree source," *IEEE J. Sel. Topics Signal Process.*, vol. 14, no. 1, pp. 118–129, Jan. 2020.
- [160] Z. Chen, M. Lu, Y. Zhou, and C. Chen, "Information synergy entropy based multi-feature information fusion for the operating condition identification in aluminium electrolysis," *Inf. Sci.*, vol. 548, pp. 275–294, Feb. 2021.
- [161] X. Xue, S. Wang, L. Zhang, Z. Feng, and Y. Guo, "Social learning evolution (SLE): Computational experiment-based modeling framework of social manufacturing," *IEEE Trans. Ind. Informat.*, vol. 15, no. 6, pp. 3343–3355, Jun. 2019.
- [162] W. Gao, W. Wang, D. Dimitrov, and Y. Wang, "Nano properties analysis via fourth multiplicative ABC indicator calculating," *Arabian J. Chem.*, vol. 11, no. 6, pp. 793–801, Sep. 2018.
- [163] R. Guan, H. Zhang, Y. Liang, F. Giunchiglia, L. Huang, and X. Feng, "Deep feature-based text clustering and its explanation," *IEEE Trans. Knowl. Data Eng.*, early access, Oct. 6, 2020, doi: [10.1109/TKDE.2020.3028943](https://doi.org/10.1109/TKDE.2020.3028943).
- [164] C. Yang, L. Bruzzone, H. Zhao, Y. Tan, and R. Guan, "Superpixel-based unsupervised band selection for classification of hyperspectral images," *IEEE Trans. Geosci. Remote Sens.*, vol. 56, no. 12, pp. 7230–7245, Dec. 2018.



TIANRU ZHU is currently pursuing the degree with the School of the 2nd Clinical Medical Sciences, Wenzhou Medical University. His main research interest includes medical diagnosis.



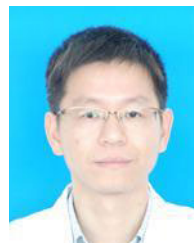
ZHONGXIANG XIAO received the M.S. degree in medical science from Wenzhou Medical University, China, in 2009. He is currently an Associate Chief Pharmacist with the Department of Pharmacy, Affiliated Yueqing Hospital, Wenzhou Medical University. His main research interests include therapeutic drug monitoring, clinical pharmacology, and inflammatory diseases.



XIE ZHANG received the master's degree in medicine from Wenzhou Medical University, in 2013. He is currently with the Department of Pulmonary and Critical Care Medicine, Affiliated Yueqing Hospital, involved in clinical treatment, scientific research, and education of respiratory medicine.



LONG ZHENG is currently an Attending Physician with the Department of Pulmonary and Critical Care Medicine, Affiliated Yueqing Hospital, Wenzhou Medical University. His main research interest includes respiratory infectious diseases.



RONGWEI ZHENG is currently the Deputy Chief Physician with the Department of Urology, Affiliated Yueqing Hospital, Wenzhou Medical University. His field of study is urinary tract infections in critically ill patients.



YANGJIE SUN received the master's degree in medicine in 2019. She is currently a Resident with the Department of Pulmonary and Critical Care Medicine, Affiliated Yueqing Hospital, Wenzhou Medical University.



HUA YE received the M.S. degree in medical science from Wenzhou Medical University, China, in 2017. She is currently the Chief Physician with the Department of Pulmonary and Critical Care Medicine, Affiliated Yueqing Hospital, Wenzhou Medical University. Her main research interests include respiratory infectious diseases and lung tumors.



PEILIANG WU received the M.S. degree in medical science from Wenzhou Medical University, China, in 2017, where he is currently pursuing the Ph.D. degree in respiratory medicine. He is currently a Resident Physician with the Department of Pulmonary and Critical Care Medicine, The 1st Affiliated Hospital, Wenzhou Medical University. His main research interests include respiratory infectious diseases, lung cancer, and pulmonary arterial hypertension.



WEILONG ZHOU is currently a Chief Physician with the Department of Pulmonary and Critical Care Medicine, Affiliated Yueqing Hospital, Wenzhou Medical University. Her main research interest includes respiratory infectious diseases.



QINLEI FU received the M.S. degree in medical science from Wenzhou Medical University, China, in 2019. He is currently a Resident Physician with the Department of Pulmonary and Critical Care Medicine, Affiliated Yueqing Hospital, Wenzhou Medical University. His main research interest includes respiratory infectious diseases.



XINXIN YE received the master's degree in medicine in 2019. He is currently a Resident with the Department of Pulmonary and Critical Care Medicine, Affiliated Yueqing Hospital, Wenzhou Medical University.



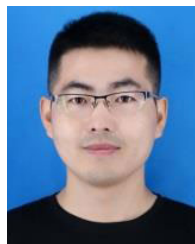
ALI CHEN received the master's degree majoring in respiratory medicine from Wenzhou Medical University, in 2017. She is currently a Respiratory Physician with the Yueqing People's Hospital, Wenzhou, Zhejiang, in China. Her main research interests include chronic obstructive pulmonary disease and pulmonary arterial hypertension.



SHUANG ZHENG received the M.S. degree in medical science from Wenzhou Medical University, China, in 2017. She is currently a Resident Physician with the Department of Pulmonary and Critical Care Medicine, Affiliated Yueqing Hospital, Wenzhou Medical University. Her main research interest includes respiratory infectious diseases.



ALI ASGHAR HEIDARI He is currently a Ph.D. Research Intern with the School of Computing, National University of Singapore. He is currently pursuing the Ph.D. degree with the University of Tehran. He was supported by the National Elites Foundation, Iran. He has authored or coauthored more than 20 articles in prestigious international journals, such as *Information Fusion*, *Information Sciences*, *Future Generation Computer Systems*, *Energy Conversion and Management*, *Applied Soft Computing*, *Knowledge-Based Systems*, and *Expert Systems With Applications*. His main research interests are advanced machine learning, evolutionary computation, meta-heuristics, prediction, information systems, and spatial modeling.



MINGJING WANG is currently a Special Researcher with the Institute of Research and Development, Duy Tan University, Da Nang, Vietnam. His research interests are data mining, machine learning, evolutionary computation, and their applications to medical diagnosis. He has authored or coauthored several articles in the field of computer engineering in top-ranking journals, such as *Neurocomputing*, the *Engineering Applications of Artificial Intelligence*, *Energy Conversion and Management*, *Applied Mathematical Modelling*, and *Applied Soft Computing*.



JIANDONG ZHU is currently the Chief Physician with the Department of Oncology, Affiliated Yueqing Hospital, Wenzhou Medical University, where he holds the position of Vice President of function. His research fields are lung cancer and thyroid cancer.



HUILING CHEN (Associate Member, IEEE) received the Ph.D. degree from the Department of Computer Science and Technology, Jilin University, China. He is currently an Associate Professor with the College of Computer Science and Artificial Intelligence, Wenzhou University, China. He has authored or coauthored more than 100 papers in international journals and conference proceedings, including *Information Sciences*, *Pattern Recognition*, *Future Generation Computer System*, *Expert Systems With Applications*, *Knowledge-Based Systems*, *Applied Soft Computing*, *Neurocomputing*, and *PAKDD*. His current research interests center on machine learning, data mining, and their applications to medical diagnosis and bankruptcy prediction. He is currently serving as an Associate Editor for IEEE Access. He is also a Reviewer for many journals, such as *Applied Soft Computing*, *Artificial Intelligence in Medicine*, *Knowledge-Based Systems*, and *Future Generation Computer System*. He is ranked worldwide among top scientists for computer science and electronics prepared by Guide2Research, one of the leading portals for computer science research. <https://guide2research.com/u/huiling-chen>.



JIFA LI is currently the Chief Physician with the Department of Pulmonary and Critical Care Medicine, Affiliated Yueqing Hospital, Wenzhou Medical University. His research interests include respiratory chronic interstitial diseases, respiratory tract infectious diseases, and lung tumors.

...